PRAMANA
— journal of
physics

© Printed in India

Vol. 43, No. 3,
September 1994
pp. 193–199

Investigation of phonon anomalies in intermediate valence compounds SmS and $Sm_{0.75}Y_{0.25}S$

PRAFULLA KUMAR JHA and SANKAR P SANYAL
Department of Physics, C V Raman Building, Barkatullah University, Bhopal 462026, India

MS received 2 April 1994; revised 4 July 1994

Abstract. Phonon anomalies in two intermediate valence compounds (IVC), SmS and $Sm_{0.75}Y_{0.25}S$ have been investigated using breathing shell model (BSM). The BSM includes breathing motion of electron shells of the rare earth atom due to $f-d$ hybridization. The phonon dispersion curves of IVC, calculated from the present model, agree well with the measured data. One-phonon density of states calculated from the present model compares well with the Raman spectra.

Keywords. Phonons; phonon dispersion curves; dynamical matrix; density of states.

PACS Nos 63·20; 63·10

1. Introduction

The valence instability of the intermediate valence (IV) systems due to fluctuations between the $4f^n$ and $4f^{n+1}$ electronic configurations gives rise to peculiar phonon properties [1–11]. Because of this large volume difference in the two electronic states, strong electron-phonon interactions have been observed in these systems [1, 4, 8–9]. These volume fluctuations or the breathing motion of the electron shells of rare earth atoms occur on a time scale comparable with lattice response time, which influence on the phonon properties such as damping or softening of the phonon modes and elastic constants. Some of the IV compounds (IVC) for which phonon properties have been studied are sulfides and selenides of samarium (Sm), thulium (Tm) and yttrium (Y) and their alloys [5, 8–9, 11–14].

The phonon anomalies common to almost all the IVCs consist of softening of the zone boundary longitudinal phonon modes. For SmS in its semiconductor state, it is the longitudinal optical (LO) branch which gets soft at the zone boundary [8–9] while for $Sm_{0.75}Y_{0.25}S$ and YS both LO and LA show softening near the zone boundary. Similar situation is also observed in TmSe [1, 4]. The strong electron-phonon interactions which arise due to volume fluctuations affect the elastic properties of the IVCs. In SmS, C_{12} is small [6, 15] while in TmSe, YS and $Sm_{0.75}Y_{0.25}S$ it is negative [8, 9].

Recently much effort has been put in to interpret the electron-phonon interactions in IVCs namely SmS, $Sm_{0.75}Y_{0.25}S$, YS and TmSe [8–11]. Guntherodt *et al* [8] have examined the phonon anomalies in SmS, $Sm_{0.75}Y_{0.25}S$ and YS by using a lattice dynamical theory which considers the interionic charge deformabilities [8]. This theory satisfactorily explained the mode softening and Raman spectrum in these solids. The phonon dispersion curves (PDC) for YS and TmSe were measured long

back [2] where the PDC has been analysed using the rigid ion model. Only limited information is available for the optical modes in TmSe while no complete measurements of PDC for SmS is reported so far [1]. These authors have emphasized the necessity of a model theory which considers the charge deformabilities [2]. The phenomenological approach of Bilz *et al* [9] based on adiabatic cluster deformation of RE ion site seems to be the most successful one but the drawback with this approach is the fitting of the parameters with the PDC. In a recent paper Mischenko and Kikoin [11] have considered the contribution from charge density deformation and microscopic theory of electron-phonon interaction in IVCs. We have also reported the calculated results on PDC and one-phonon density of states using three-body force rigid ion model (TRIM) [1], which considers the long range many body interactions arises due to charge transfer between neighbor ions. This model explain the optical branches but fails to explain the acoustic anomalies in TmSe.

The phonon models mentioned above have considerable drawback, as far as their predictions are concerned. All the model theories fit their model except our own TRIM [1] to the measured dispersion curves to achieve a least square fit without taking care of the physical significance of the magnitudes of the fitted parameters.

In the present paper we report the results of the theoretical calculations of the PDC and one phonon density of states of SmS and $Sm_{0.75}Y_{0.25}S$ using a lattice dynamical model theory which includes the breathing motion of the valence electrons of the RE ions. This breathing motion of electron shells arises due to $f-d$ hybridization. This model has already been used to interpret the phonon properties in U-compounds which show similar phonon anomalies [16, 17].

2. Theory

The breathing shell model (BSM) considers phenomenologically the short range electron–phonon interactions in terms of electron shell deformations. Depending upon symmetry, it includes dipolar, quadrupolar and breathing deformabilities of the electron shells of the polarizable ions. A detailed review of this model can be obtained from [15, 18].

The dynamical matrix derived from the interaction hamiltonian can be written as [15]

$$D(q) = (R' + \mathrm{ZCZ}) - (R' + \mathrm{ZCY})(R' + K + \mathrm{YCY})^{-1}(R' + \mathrm{YCZ}) \tag{1}$$

where

$$R' = (R - QH^{-1}Q^{+}). \tag{2}$$

Here C and R are the coulomb and short range repulsive interaction matrices. Q is a (6×2) matrix representing the breathing mode variable while H is a (2×2) matrix specifying the interactions between the breathing mode variables of different ions in the lattice. K and Y are the diagonal matrices and represent the core–shell interaction and shell charge respectively.

The present version of the BSM has altogether eight parameters, which can be self consistently determined from elastic, dielectric and zone centre phonon properties. However, since we have not made any attempt to obtain the least square fit to the phonon data, we have assumed $Y = Y_1 = Y_2$ to minimize the number of parameters. The input and model parameters are listed in tables 1 and 2.

Table 1. Input parameters for SmS and $Sm_{0.75}Y_{0.25}S$.

Property	Value	
	SmS	$Sm_{0.75}Y_{0.25}S$
a	5·975	5·695
C_{11}	1·25	$1·129 \pm 0·70$
C_{12}	0·12	−0·491
C_{44}	0·31	0·299
$\nu_{TO}(\Gamma)$	5·33	7·900
α_1	0·41	0·45
α_2	5·50	6·50
ε_0	3·55	6·45
ε_∞	9·69	6·45

Elastic constants are in 10^{12} dyn/cm^2, frequency in THz, a in Å and polarizability in Å^{-3} [2, 8, 14].

Table 2. Model parameters for IVC using BSM. All are in units of $e^2/2V$ except Y which is in units of e.

Parameters	Value	
	SmS	$Sm_{0.75}Y_{0.25}S$
A_{12}	50·17260	15·53927
B_{12}	−8·66930	2·76889
A_{11}	12·77000	−1·70398
B_{11}	−3·17000	0·40826
B_{22}	−10·36000	3·63200
G_1	826·45000	11130·43900
G_2	33·04620	926·11500
Y	−2·49000	−9·82170

3. Results and discussion

The calculated phonon dispersion curves for SmS and $Sm_{0.75}Y_{0.25}S$ are plotted in figures 1 and 2 and compared with experimental results [2, 8, 11]. In figure 1 we have presented the PDC for SmS using BSM. The figure reveals that the BSM can explain satisfactorily the measured acoustic branches all along the Brillouin zone. The optical branches particularly in Δ and Λ directions are reproduced well by the present model while it fails in predicting the phonon modes in Σ direction. Since the information about the longitudinal optical branches is limited, appropriate comment cannot be made.

The calculated phonon dispersion curves for $Sm_{0.75}S_{0.25}S$ obtained from the present model are presented in figure 2 and compared with the neutron scattering measurements [8]. Since the model does not consider the doping effect of yttrium hence the local mode at 5·2 THz has not been shown in the figure, similar to what has been

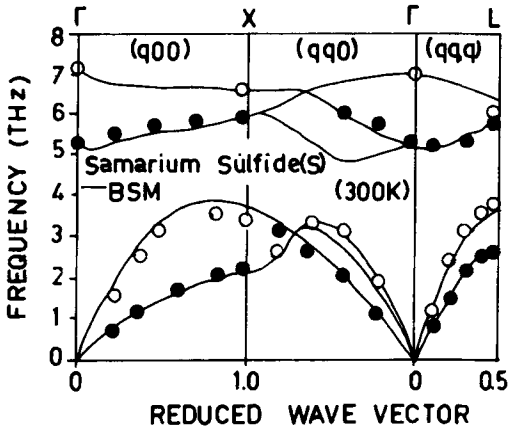

Figure 1. Phonon dispersion curves for SmS. Experimental points are taken from ref. [2, 8, 11].

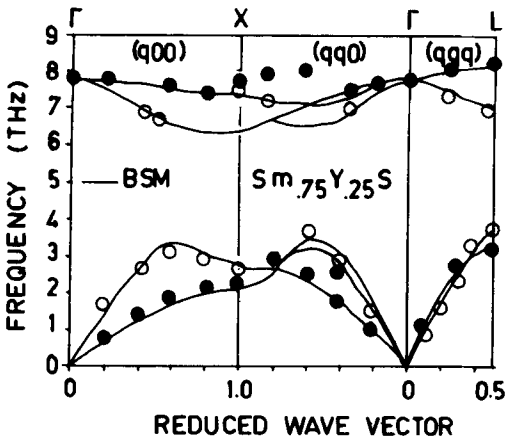

Figure 2. Same as in figure 1 for $Sm_{0.75}Y_{0.25}S$. Experimental points are taken from [2, 8].

reported by Mischenko and Kikoin [11]. Figure 2 reveals that the acoustic branches in $Sm_{0.75}Y_{0.25}S$ alloy have been fairly well reproduced by the present model. In this compound the BSM has predicted fairly well the longitudinal acoustic phonon anomalies throughout the Brillouin zone (BZ). The softening of LA branch at X-point, fairly close magnitude of LA and TA_2 modes along Σ direction particularly at lower wave vectors, softening of LA branch and crossing over TA around (0·4, 0·4, 0·4) have been explained satisfactorily. On the other hand the present model fails to predict the optical branches satisfactorily.

The force constants presented in table 2 for SmS and $Sm_{0.75}Y_{0.25}S$ are reasonably physical. The parameters are physically significant, in the sense that they correctly reproduce the short-range interactions and the crystal properties of these solids. These physically reasonable force constants have been obtained from the macroscopic properties of these compounds. From table 2 it is clear that the positive and negative ion interaction is dominant. The positive–positive ion and negative–negative ion

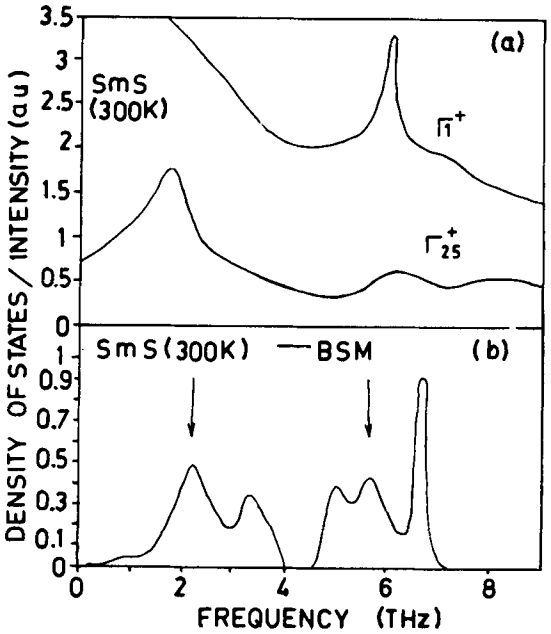

Figure 3. (a) One phonon Raman spectrum of SmS [2, 8]. (b) One phonon density of States of SmS.

interactions are small in magnitude. The $Sm_{0.75}Y_{0.25}S$, however do not follow the trend as SmS. This can be justified from the fact that the dispersion curves for $Sm_{0.75}Y_{0.25}S$ quantitatively reveal metallic nature and zone centre LO and TO phonons degenerate, while the same for SmS are different.

In figure 3, we have presented the one-phonon density of states (DOS) for SmS and compared with Raman spectrum [8]. The experimental Raman spectrum excludes the contribution due to quadrupolar deformability (Γ_{12}^+). Guntherodt *et al* [8] have observed a peak at 6 THz (200 cm^{-1}), contributed by zone boundary LO phonons due to breathing deformabilities. In our DOS, we have also observed similar peak at 6·25 THz contributed by the longitudinal phonons only. The largest contributions arise from the L point of the Brillouin Zone. This result is similar to EuS [20]. However, $q = 0$ phonons are observed at 300 K in EuS due to spin disorder, whereas due to lattice defects in SmS [7]. Another peak in the higher frequency side is due to TO branches. The broad band below 4 THz in figure 3 is from acoustic phonons and can be verified from the experimental Raman spectrum which is attributed to first order defect induced Raman scattering from acoustic phonons. It seems, therefore, the present model has predicted the gross features of the density of states for SmS.

In figure 4, we compare the DOS and Raman spectrum for $Sm_{0.75}Y_{0.25}S$. The Raman spectra of $Sm_{0.75}Y_{0.25}S$ show two sharp peaks at 2·5 THz and 7·0 THz which are due to the Sm- breathing deformability. The density of states of $Sm_{0.75}Y_{0.25}S$ calculated from the present model predicts the peaks at 7·0 THz contributed by LO phonons. This peak could be verified from the Raman spectrum. In our calculated density of states, we have also observed a peak at 6·25 THz due to TO phonons. In $Sm_{0.75}Y_{0.25}S$ the DOS shows a gap between 3·75 THz and 5·75 THz due to the separation between optical and acoustical branches. The peak at 2·55 THz in the

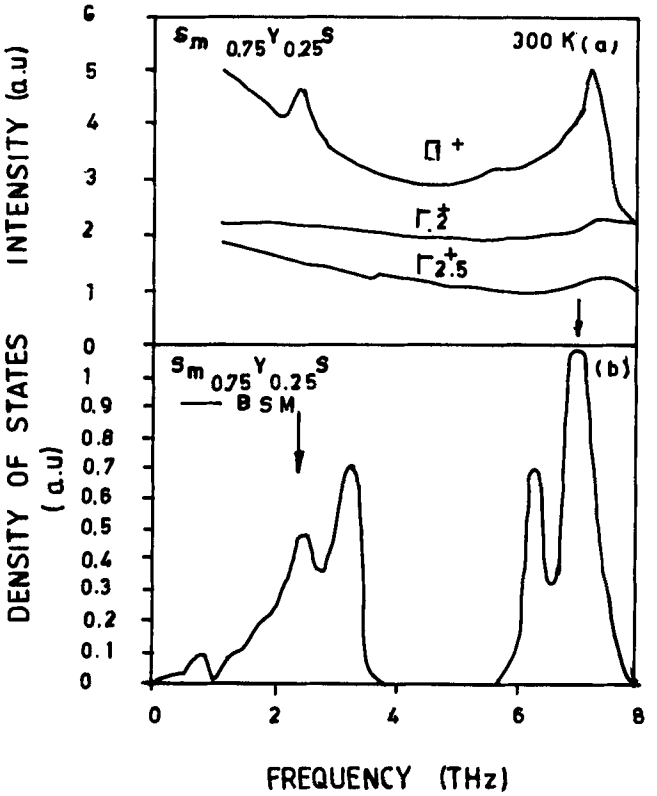

Figure 4. Same as in figure 3 for $Sm_{0.75}Y_{0.25}S$ [8].

lower frequency region of the Raman spectrum could also be obtained from our calculated DOS.

Therefore, from figures 3 and 4 it seems that the breathing deformability of Sm ion is responsible for the dominant contributions of Γ_2^+ Raman scattering and LO(L) phonons in the SmS and LO(L) and LA(L) in $Sm_{0.75}Y_{0.25}S$ to the peak at higher frequency side of the DOS.

Finally, in the present paper we have presented the results of a systematic study of phonon properties of SmS and $Sm_{0.75}Y_{0.25}S$. The calculated results bring out the views that the phonon anomalies in these compounds, in general originates from the breathing motion of the electron shells of rare earth ions. The breathing shell model satisfactorily reproduces the gross feature of the PDC. These predictions reveal that the short range deformations due to breathing motion of the electron shells of RE ions contribute significantly to the phonon anomalies in IVCs.

Acknowledgements

The work is financially supported by DAE, Government of India. One of us (PKJ) acknowledges the award of Research Associateship from CSIR, New Delhi.

References

[1] P K Jha and S P Sanyal, *Indian J. Pure Appl. Phys.* **31**, 469 (1993)
[2] H A Mook and F Holtzberg, *Valence fluctuations in solids*, edited by L M Falicov, W Hanke and M B Maple (North Holland, Amsterdam, 1981), p 113 and references therein
[3] H A Mook and R M Nicklov, *Phys. Rev.* **B20**, 1656 (1977)
[4] H A Mook, R M Nicklov, T Penny, F Holtzberg and W Shafer, *Phys. Rev.* **B18**, 2925 (1979)
[5] H A Mook, D B Mc Wahn and F Holtzberg, *Phys. Rev.*, **B25**, 4321 (1982)
[6] A Jayaraman, V Narayanamurti, E Bucher and R G Mains, *Phys. Rev. Lett.* **24**, 1430 (1970)
[7] G Guntherodt, R Merlin, A Frey and M Cardona, *Solid State Commun.* **27**, 251 (1978)
[8] G Guntherodt, A Jayaraman, W Kress and H Bilz, *Phys. Rev. Lett.* **20**, 824 (1981)
[9] H Bilz, G Guntherodt, W Klippmann and W Kress, *Phys. Rev. Lett.* **43**, 1998 (1979)
[10] P Roedhammer, W Reichardt and F Holtzberg, *Phys. Rev. Lett.* **40**, 465 (1978)
[11] A S Mischenko and K A Kikoin, *J. Phys. Condensed Matter.* **3**, 5937 (1991)
[12] H Boppart, A Treindl and P Wachter, *Valence Fluctuations in Solids*, edited by L M Falicov, W Hanke and M B Maple (North Holland, Amsterdam, 1981), p 103 and references therein
[13] P K Jha and S P Sanyal, *Indian J. Pure Appl. Phys.* **31**, 762 (1993)
[14] S P Sanyal and V Mishra, *Indian J. Pure Appl. Phys.* **26**, 624 (1988)
[15] V Nusslein and U Schroder, *Phys. Status Solidi.* **B21**, 309 (1967)
[16] P K Jha and S P Sanyal, *Phys. Rev.* **B** (1993) (in press)
[17] P K Jha and S P Sanyal, *Pramana – J. Phys.* **42**, 9 (1993)
[18] R K Singh, *Phys. Rep.* **85**, 259 (1982)
[19] T Hailing, G S Saunders and H Back, *Phys. Rev.* **B29**, 1848 (1984)
[20] R Merlin, R Zeyher and G Guntherodt, *Phys. Rev. Lett.* **39**, 1215 (1977)